Inverse Problems in Image Processing

Ramesh Neelamani (Neelsh)

Committee: Profs. R. Baraniuk, R. Nowak, M. Orchard, S. Cox

June 2003

Inverse Problems

- Data estimation from inadequate/noisy observations
  - Oft-encountered in practice
- Non-unique solution due to noise and lack of information
- Reduce ambiguity by exploiting structure of desired solution
  - Piece-wise smooth structure of real-world signals/images
  - Lattice structures due to quantization

Image Processing Inverse Problems

- Deconvolution: restore blurred and noisy image
  - Exploit piece-wise smooth structure of real-world signals
  - Applications: most imaging applications
- Inverse halftoning: obtain gray shades from black & white image
  - Exploit piece-wise smooth structure of real-world signals
  - Applications: binary image recompression, processing faxes
- JPEG Compression History Estimation (CHEst) for color images
  - Exploit inherent lattice structures due to quantization
  - Applications: JPEG recompression, artifact removal

Deconvolution

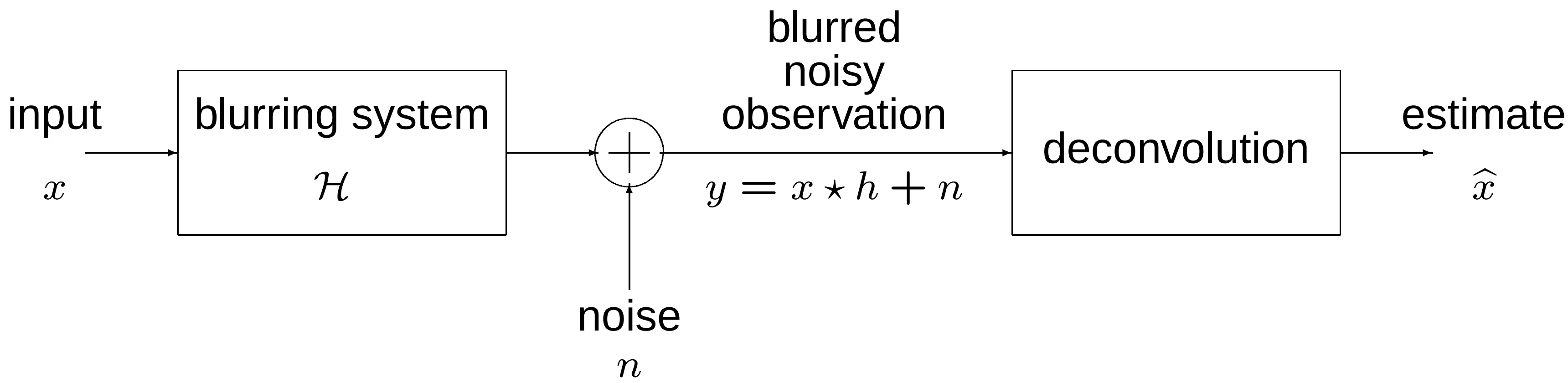

input

observed

estimate

- Problem: $y = x \star h + n$; given y, h, find x
- Applications: most imaging applications (seismic, medical, satellite)

Deconvolution is Ill-Posed

blurred noisy image $Y(f) = X(f)H(f) + N(f)$ → inverse $\mathcal{H}^{-1}$ → $X(f) + \frac{N(f)}{H(f)}$ deconvolution estimate

$|H(f)|$

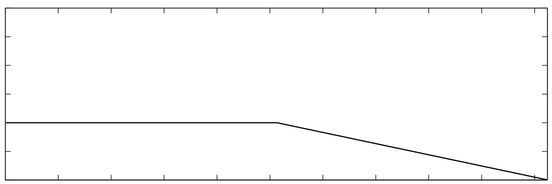

frequency f

$|H^{-1}(f)|$

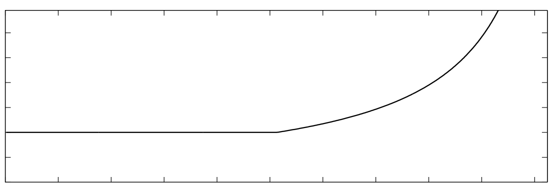

frequency f

after pure inversion

- $|H(f)| \approx 0 \;\Rightarrow\;$ noise $\frac{N(f)}{H(f)}$ explodes!
- Solution: *regularization* (approximate inversion)

Fourier-Wavelet Regularized Deconvolution (ForWaRD)

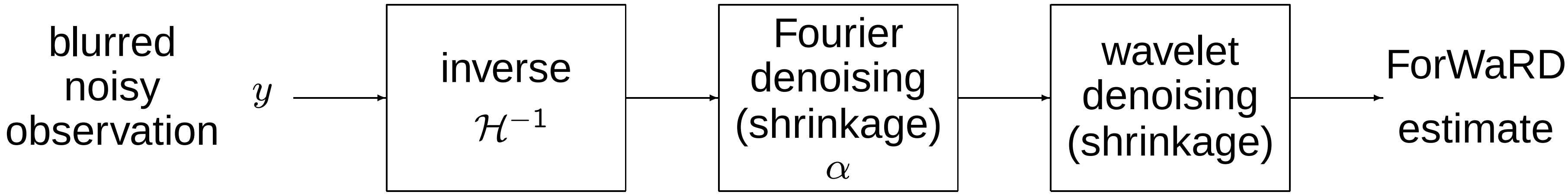

- Fourier denoising: exploits colored noise structure

  Wavelet denoising: exploits input signal structure

- Choice of α: balance Fourier and wavelet denoising
  - Optimal $\alpha \rightarrow$ economics of signal's wavelet representation

- Applicable to all convolution operators

- Simple and fast algorithm: $O(M \log^2 M)$ for M pixels

Asymptotic ForWaRD Properties

- Theorem: Let signal $x \in$ Besov space $B^s_{p,q}$ (i.e., piece-wise smooth signals), Tikhonov reg. parameter $\alpha > 0$ (fixed), and "smooth" $|H(f)|$. Then as the number of samples M increases,

Wavelet shrinkage error	$\downarrow$	$M^{\frac{-2s}{2s+1}}$ (fast decay)
Fourier shrinkage error	$\rightarrow$	constant determined by α (bias)

- ForWaRD improves on WVD at small samples

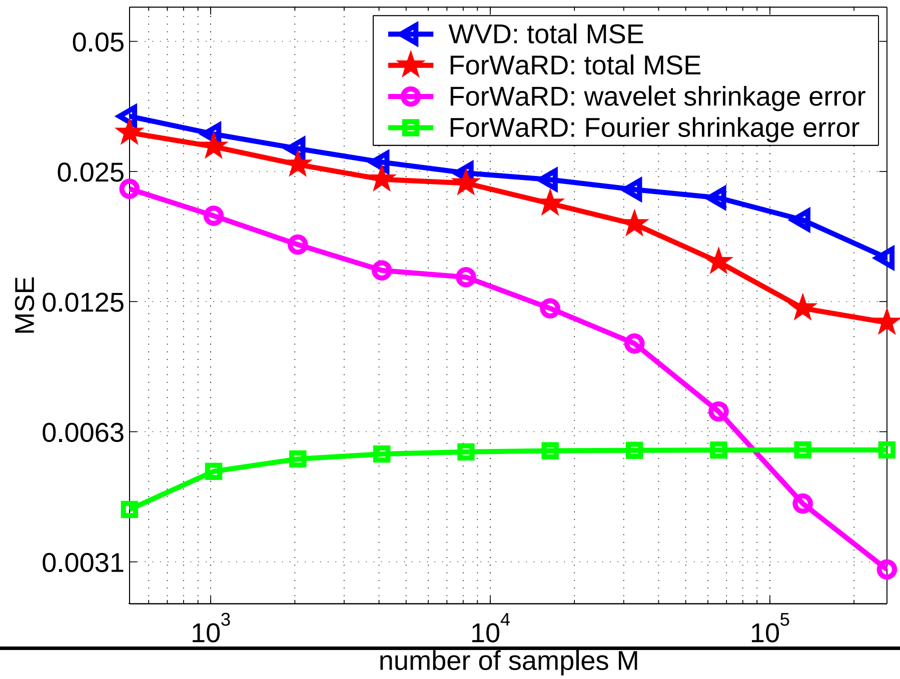

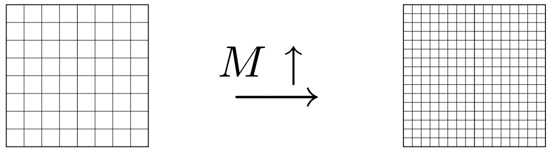

Asymptotic ForWaRD Optimality

- Theorem: Let signal $x \in$ Besov space $B^s_{p,q}$ and $\mathcal{H}$ be a "scale-invariant" operator; that is, $|H(f)| \propto |f|^{-\nu}, \nu > 0$. If

  $$\text{Tikhonov parameter } \alpha \leq M^{-\beta},$$

  $$\text{where } \beta > \frac{s}{2s+2\nu+1} . \max\left(1, \frac{4\nu}{\min\left(2s, 2s+1-\frac{2}{p}\right)}\right),$$

  then, as the number of samples M increases,

  $$\text{ForWaRD MSE} \quad \downarrow \quad M^{\frac{-2s}{2s+2\nu+1}}.$$

  Further, no estimator can achieve a faster error decay rate than ForWaRD for every $x(t) \in B^s_{p,q}$.

- ForWaRD enjoys the same asymptotic optimality as the WVD

Image Deconvolution Results

Original

Observed (9x9, 40dB BSNR)

Wiener (SNR = 20.7 dB)

ForWaRD (SNR = 22.5 dB)

ForWaRD: Conclusions

- ForWaRD: balances Fourier-domain and wavelet-domain denoising
- Simple $O(M \log^2 M)$ algorithm with good performance.
- Ph.D. Contributions:
  - Asymptotic ($M \to \infty$) error analysis for most operators
  - Asymptotic optimality results for scale-invariant operators
- Status: IEEE Trans. on Signal Processing (to appear)
- Collaborators: H. Choi and R. Baraniuk

Halftoning and Inverse Halftoning

contone

halftone

- Halftoning (HT): continuous-tone (contone) $\longrightarrow$ binary (halftone)
  - Halftone visually resembles contone
  - Employed by printers, low-resolution displays, etc.
- Inverse halftoning (IHT): halftone $\longrightarrow$ contone
  - Applications: lossy halftone compression, facsimile processing
  - Many contones $\longrightarrow$ one halftone $\Rightarrow$ ill-posed problem

Inverse Halftoning ≈ Deconvolution

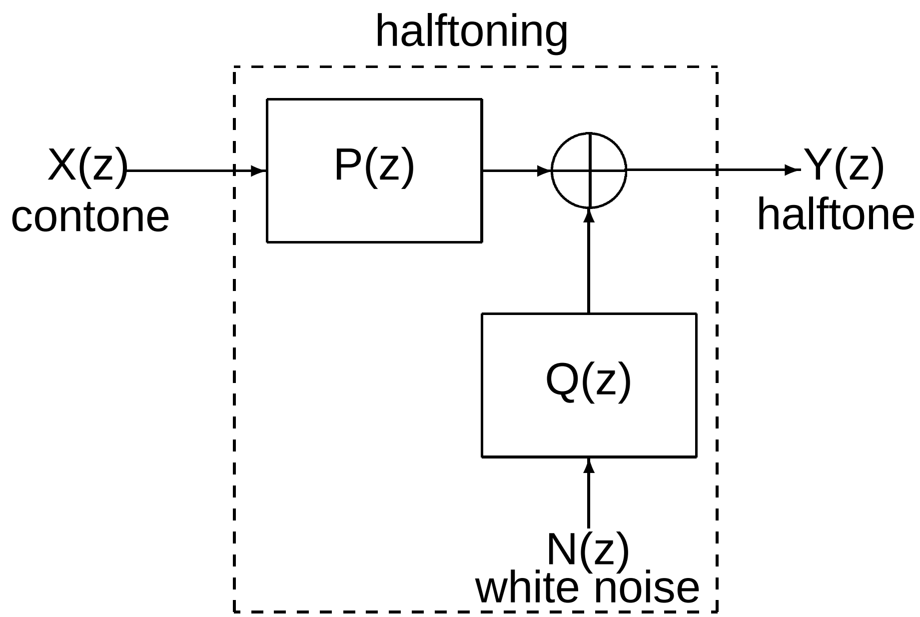

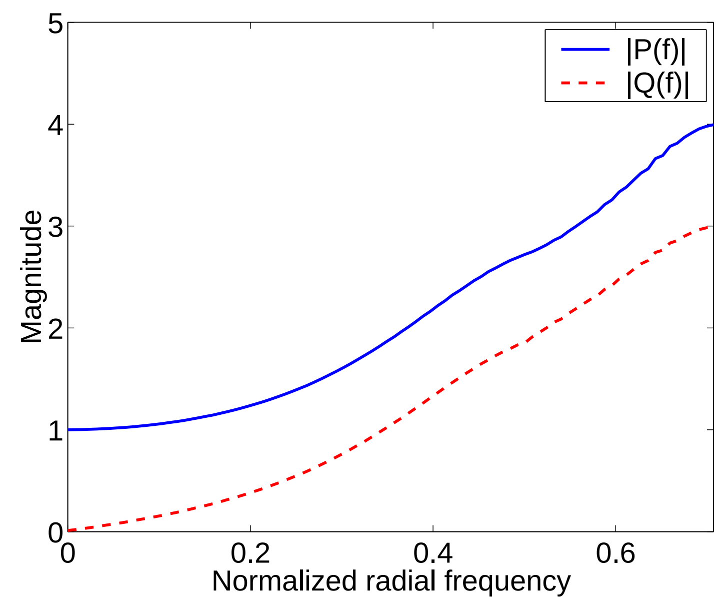

- From Kite et al. '97, $Y(z) = P(z)X(z) + Q(z)N(z)$, where $P(z) := \frac{K}{1+(K-1)H(z)}$ and $Q(z) := \frac{1-H(z)}{1+(K-1)H(z)}$

- Deconvolution: given Y, estimate X – a well-studied problem

  $\Rightarrow$ For error diffusion (ED) halftones, IHT ≈ deconvolution

Wavelet-based Inverse Halftoning Via Deconvolution (WInHD)

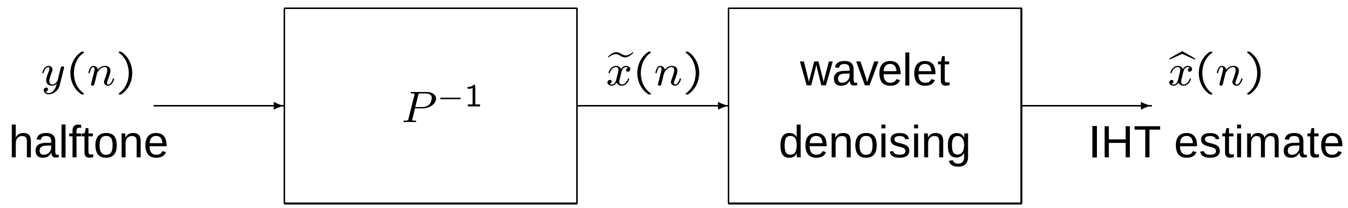

- WInHD algorithm:
  1. Invert $P(z)$: $P^{-1}(z)Y(z) = X(z) + P^{-1}(z)Q(z)\Gamma(z)$
  2. Attenuate noise $P^{-1}Q\,\Gamma$ with wavelet-domain scalar estimation
- Wavelet denoising exploits input image structure
- Computationally efficient: $O(M)$ for M pixels
- Structured solution: adapts by changing P, Q and K for different ED
  - Most existing IHT algorithms are tuned empirically

Asymptotic Optimality of WInHD

- Main assumption: accuracy of linear model for ED

- Guaranteed fast error decay with increasing spatial resolution

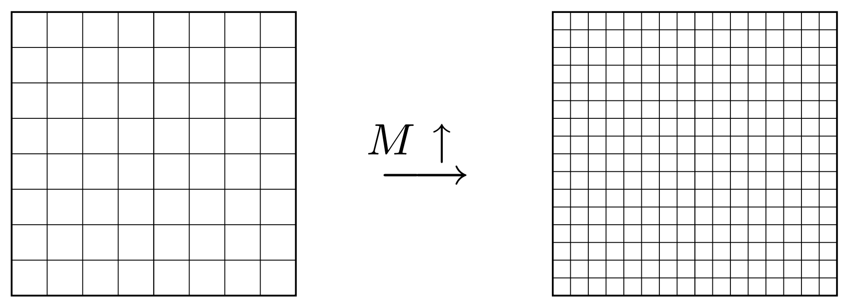

For signals in Besov space $B^s_{p,q}$, as the number of pixels $M \to \infty$,

$$\text{WInHD MSE} \downarrow M^{\frac{-s}{s+1}}.$$

- Decay rate is optimal, if original contone is noisy

Simulation Results

contone

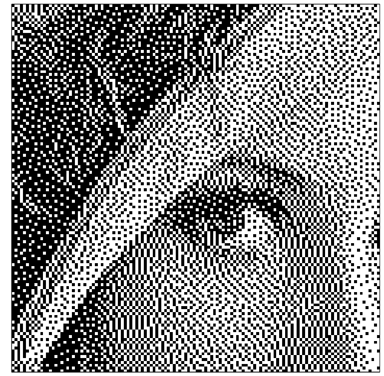

halftone

Gaussian LPF
(PSNR 28.6 dB)

Gradient [Kite ’98]
(PSNR 31.3 dB)

WVD
(PSNR 32.1 dB)

- WInHD is competitive with state-of-the-art IHT algorithms

WInHD: Conclusions

- Ph.D. Contributions:
  - Inverse halftoning $\approx$ deconvolution
  - WInHD: Wavelet-based Inverse halftoning via Deconvolution
    - $O(M)$ model-based algorithm with good performance
  - Asymptotic ($M \to \infty$) error analysis
- Status: IEEE Trans. on Signal Processing (submitted)
- Collaborators: R. Nowak and R. Baraniuk

JPEG Compression History Estimation (CHEst)

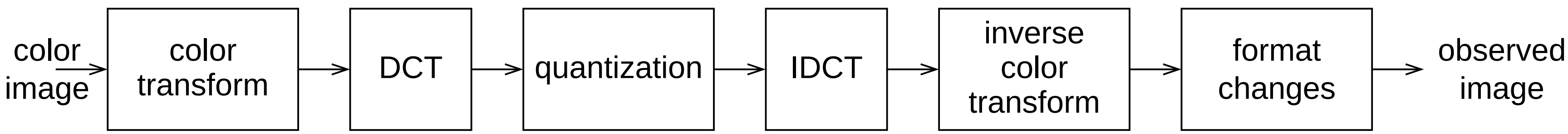

- Observed: color image that was previously JPEG-compressed
- JPEG $\longrightarrow$ TIFF or BMP: settings lost during conversion
- Desired: settings used to perform previous JPEG compression
- Applications:
  - JPEG recompression
  - Blocking artifact removal
  - Uncover internal compression settings from printers, cameras

Digital Color

- Color perceived by human visual system requires three components
- Pixel in digital color image $\longrightarrow$ 3-D vector
- Color space $\longrightarrow$ Reference frame for the 3-D vector
  - *RGB* : Red *R*, Green *G*, Blue *B*
  - *YCbCr* : Luminance *Y*, Chrominance *Cb*, Chrominance *Cr*
- Color spaces are inter-related by linear or non-linear transforms

$$\begin{bmatrix} R \\ G \\ B \end{bmatrix} = \begin{bmatrix} 1.0 & 0.0 & 1.40 \\ 1.0 & -0.344 & -0.714 \\ 1.0 & 1.77 & 0.0 \end{bmatrix} \left(\begin{bmatrix} Y \\ Cb \\ Cr \end{bmatrix} - \begin{bmatrix} 0 \\ 128 \\ 128 \end{bmatrix} \right).$$

JPEG Overview

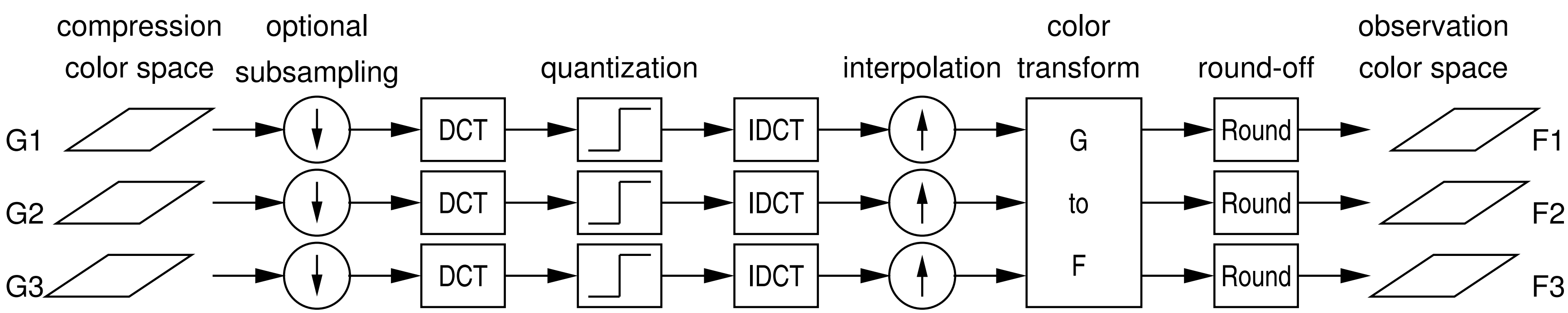

- JPEG: common standard to compress digital color images
- JPEG compression history components $\longrightarrow$ chosen by imaging device
  1. Color space used to perform compression
  2. Subsampling and complementary interpolation
  3. Quantization tables

Lattice Structure of Quantized DCT Coefficients

- 3-D vector of G space's DCT coefficients $\in$ rectangular lattice
  - $X_{G1}, X_{G2}, X_{G3} \rightarrow i^{th}$ frequency DCT coeffincents
    $q_{i,1}, q_{i,2}, q_{i,3} \rightarrow$ corresponding Q-step sizes

$$\begin{bmatrix} X_{G1} \\ X_{G2} \\ X_{G3} \end{bmatrix} \rightarrow \text{quantization} \rightarrow \begin{bmatrix} \text{round}\left(\frac{X_{G1}}{q_{i,1}}\right) q_{i,1} \\ \text{round}\left(\frac{X_{G2}}{q_{i,2}}\right) q_{i,2} \\ \text{round}\left(\frac{X_{G3}}{q_{i,3}}\right) q_{i,3} \end{bmatrix}$$

- 3-D vector of F space's DCT coefficients $\in$ parallelepiped lattice
  - Assuming no subsampling, affine G to F: F = $[\mathcal{T}]_{3\times3}$ G + Shift

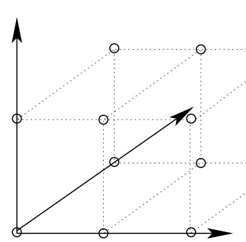

compression space G

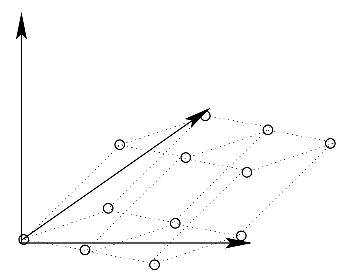

observation space F

Lattice Basis Reduction

- Given vectors b_i, lattice $\mathcal{L} := \sum_i \lambda_i\, b_i$ with $\lambda_i \in \mathbb{Z}$
- Lattice basis reduction by Lenstra, Lenstra, Jr. and Lovasz (LLL):
  - Given vectors $\in \mathcal{L}$, LLL finds an ordered set of basis vectors
    - basis vectors are nearly orthogonal
    - shorter basis vectors appear first in the order
- LLL operations are similar to Gram-Schmidt
  1. Change the order of the basis vectors
  2. Add to b_i an integral multiple of b_j
  3. Delete any resulting zero vectors

LLL Provides Parallelepiped's Basis Vectors

- Any basis for parallelepiped containing i^{th} frequency 3-D vectors

$$\mathcal{B}_i := \left[\quad \mathcal{T} \quad \right] \begin{bmatrix} q_{i,1} & 0 & 0 \\ 0 & q_{i,2} & 0 \\ 0 & 0 & q_{i,3} \end{bmatrix} \left[\quad \mathcal{U}_i \quad \right] =: \mathcal{T}\mathcal{Q}_i\mathcal{U}_i$$

$\mathcal{U}_i \in \mathbb{Z}^{3\times 3} \rightarrow$ unit-determinant matrix

- From LLL's properties, and since $\mathcal{T} \rightarrow$ nearly-orthogonal
  - LLL's $\mathcal{B}_i$'s 1^{st} (shortest) column is aligned with one of $\mathcal{T}$'s columns
  - The $\mathcal{U}_i$'s in LLL's $\mathcal{B}_i$ are "close" to identity. For example,

$$\mathcal{U}_i = \begin{bmatrix} 1 & 0 & 1 \\ 0 & 1 & 0 \\ 0 & 0 & 1 \end{bmatrix},$$

Color Transform and Q-step Sizes from Different $\mathcal{B}_i$'s

- Need to undo effect of $\mathcal{U}_i$ from $\mathcal{B}_i$ to get $\mathcal{T}\mathcal{Q}_i$
  - Choose $\mathcal{U}_i$'s such that $\mathcal{U}_i\mathcal{B}_i^{-1}\mathcal{B}_j\mathcal{U}_j^{-1}$ is diagonal
  - Obtain $\mathcal{T}\mathcal{Q}_i = \mathcal{B}_i\mathcal{U}_i^{-1}$
- Obtain the norms of each column of $\mathcal{T}$ from the different $\mathcal{T}\mathcal{Q}_i$
  - $\|(\mathcal{T}\mathcal{Q}_i)(:,k)\|_2 = q_{i,k}\|\mathcal{T}(:,k)\|_2 \Rightarrow \|(\mathcal{T}\mathcal{Q}_i)(:,k)\|_2 \in$ 1-D lattice
- Extract $\mathcal{T}$ and the quantization tables
- From DC components, estimate shift

$\Rightarrow$ Lattice basis provide color transform, quantization table

LLL + Round-off Noise Attenuation

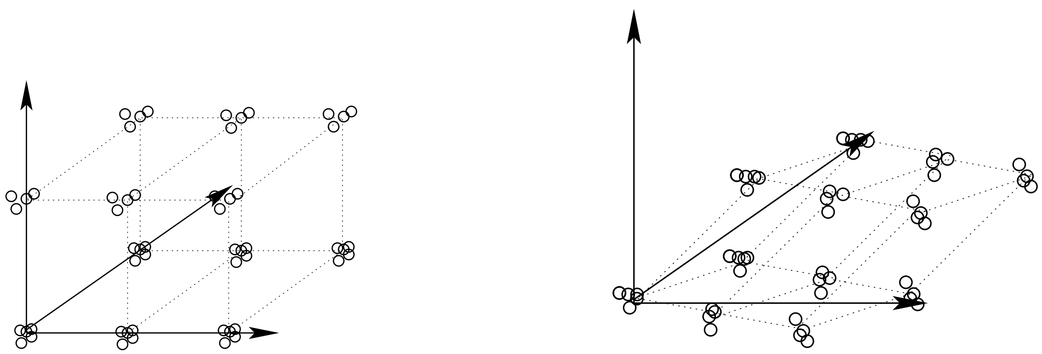

compression space G observation space F

- Round-offs perturb ideal lattice structure
- Need to incorporate noise attenuation step into LLL
  - Perform LLL with oft-occuring 3-D vectors
  - Use MAP (Gaussian round-offs) to update LLL's basis estimate
- Modified LLL provides good $\mathcal{B}_i$ estimates that help solve CHEst

Lattice-based CHEst Results (Color Transform)

- Actual color transform from *ITU.BT-601 YCbCr* space to the RGB

$$\begin{bmatrix} R \\ G \\ B \end{bmatrix} = \begin{bmatrix} 1.0 & 0.0 & 1.40 \\ 1.0 & -0.344 & -0.714 \\ 1.0 & 1.77 & 0.0 \end{bmatrix} \left(\begin{bmatrix} Y \\ Cb \\ Cr \end{bmatrix} - \begin{bmatrix} 0 \\ 128 \\ 128 \end{bmatrix} \right).$$

- Estimated color transform

$$\begin{bmatrix} R \\ G \\ B \end{bmatrix} = \begin{bmatrix} 1.00 & 0.00 & 1.41 \\ 1.00 & -0.35 & -0.71 \\ 1.00 & 1.78 & 0.00 \end{bmatrix} \left(\begin{bmatrix} Y \\ Cb \\ Cr \end{bmatrix} - \begin{bmatrix} 3 \\ 88 \\ 138 \end{bmatrix} \right)$$

- Error in shift's estimate does not affect recompression, enhancement

- $\mathcal{T}$'s estimate is very accurate

Lattice-based CHEst Results (Quantization Table)

10	7	6	10	14	24	31	$\times$
7	7	8	11	16	35	36	33
8	8	10	14	24	34	$\times$	$\times$
8	10	13	17	31	$\times$	$\times$	$\times$
11	13	22	34	41	$\times$	$\times$	$\times$
14	21	$\times$	$\times$	$\times$	$\times$	$\times$	$\times$
$\times$	$\times$	$\times$	$\times$	$\times$	$\times$	$\times$	$\times$
$\times$	$\times$	$\times$	$\times$	$\times$	$\times$	$\times$	$\times$

Y plane

10	11	14	28	$\times$	$\times$	$\times$	$\times$
11	13	16	$\times$	$\times$	$\times$	$\times$	$\times$
14	16	$\times$	$\times$	$\times$	$\times$	$\times$	$\times$
$\times$	$\times$	$\times$	$\times$	$\times$	$\times$	$\times$	$\times$
$\times$	$\times$	$\times$	$\times$	$\times$	$\times$	$\times$	$\times$
$\times$	$\times$	$\times$	$\times$	$\times$	$\times$	$\times$	$\times$
$\times$	$\times$	$\times$	$\times$	$\times$	$\times$	$\times$	$\times$
$\times$	$\times$	$\times$	$\times$	$\times$	$\times$	$\times$	$\times$

Cb plane

10	11	14	28	$\times$	$\times$	$\times$	$\times$
11	13	16	$\times$	$\times$	$\times$	$\times$	$\times$
14	16	$\times$	$\times$	$\times$	$\times$	$\times$	$\times$
$\times$	$\times$	$\times$	$\times$	$\times$	$\times$	$\times$	$\times$
$\times$	$\times$	$\times$	$\times$	$\times$	$\times$	$\times$	$\times$
$\times$	$\times$	$\times$	$\times$	$\times$	$\times$	$\times$	$\times$
$\times$	$\times$	$\times$	$\times$	$\times$	$\times$	$\times$	$\times$
$\times$	$\times$	$\times$	$\times$	$\times$	$\times$	$\times$	$\times$

Cr plane

- All estimated step sizes are exact! ($\times \rightarrow$ cannot estimate)

Dictionary-based CHEst

- Lattice-based CHEst $\longrightarrow$ affine color transform, no subsampling
- Dictionary-based CHEst $\longrightarrow$ all types of color transforms, subsampling
- Uses MAP to estimate compression history
  - Based on model for quantized coefficients + round-off noise
  - Model: given q, PDF = $\sum_k$ truncated Gaussians(kq, σ^2)

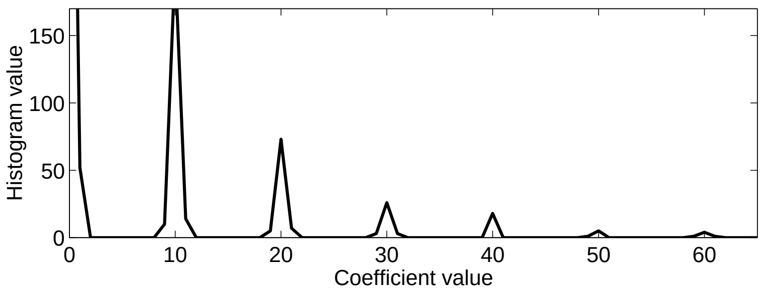

- Also yields excellent CHEst results

JPEG Recompression Using CHEst Results

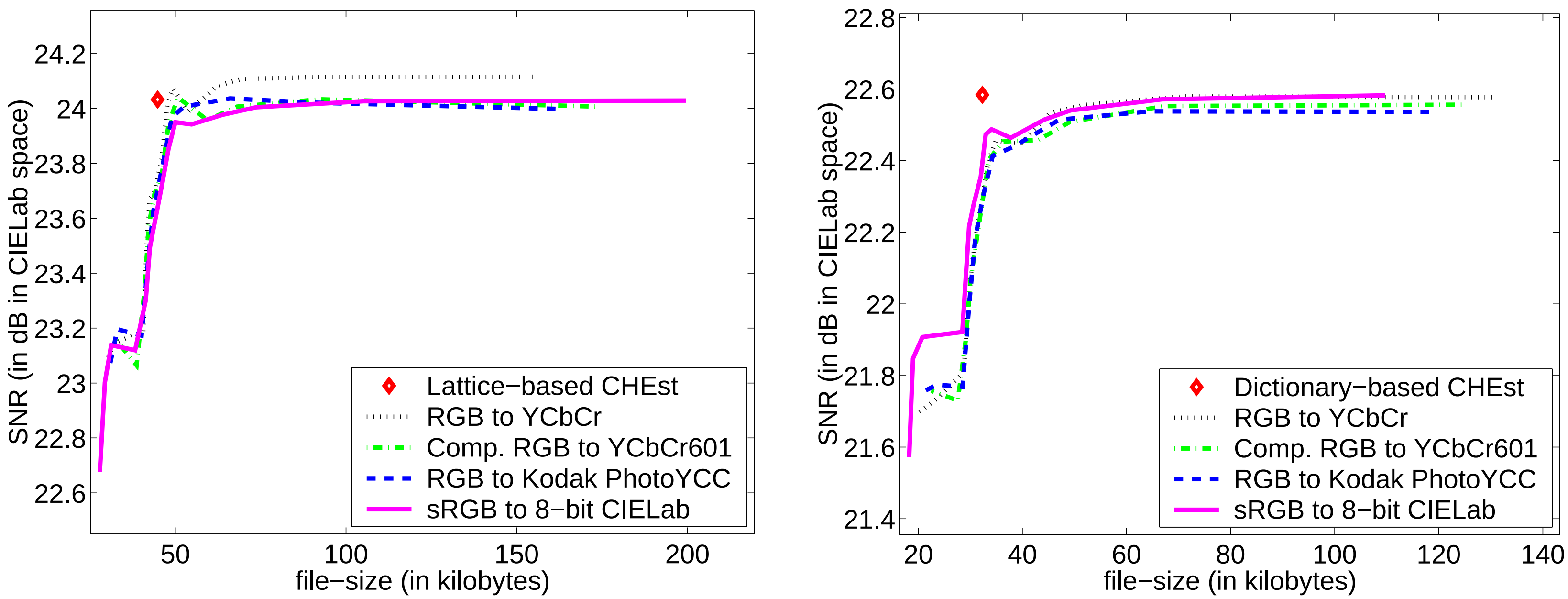

- Aim: recompress a previously JPEG-compressed BMP image
- Naive recompression $\longrightarrow$ large file-size or distortion
- CHEst results $\longrightarrow$ good file-size–distortion trade-off

JPEG CHEst: Conclusions

- Ph.D. Contributions:
  - Formulation of JPEG CHEst for color images
  - Linear case: LLL algorithm to exploit 3-D lattice structures
  - General case: MAP approach to exploit 1-D lattice structure
  - Demonstrated JPEG CHEst's utility in recompression
- Status: IEEE Trans. on Image Processing (to be submitted)
- Collaborators: R. de Queiroz, Z. Fan, and R. Baraniuk

Inverse Problems in Image Processing: Conclusions

- Deconvolution using ForWaRD:
  - Exploits piece-wise smoothness of real-world signals
  - Demonstrates desirable asymptotic performance
- Inverse halftoning using WInHD:
  - Exploits piece-wise smoothness of real-world signal
  - Demonstrates desirable asymptotic performance
- Lattice-based and Dictionary-based JPEG CHEst for color images:
  - Exploit lattice structures created due to JPEG's quantization step
  - Enables effective JPEG recompression